

KERNFORSCHUNGSZENTRUM

KARLSRUHE

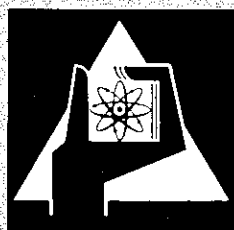
März 1972

KFK 1557

Institut für Angewandte Reaktorphysik
Projekt Schneller Brüter

Calculation of Heterogeneous Fluxes, Reaction Rates and
Reactivity Worths in the Plate Structure of Zero Power
Fast Critical Assemblies

P. E. Mc Grath, E. A. Fischer



GESELLSCHAFT FÜR KERNFORSCHUNG M. B. H.

KARLSRUHE

KERNFORSCHUNGSZENTRUM KARLSRUHE

März 1972

KFK 1557

Institut für Angewandte Reaktorphysik

Projekt Schneller Brüter

Calculation of Heterogeneous Fluxes, Reaction Rates and
Reactivity Worths in the Plate Structure of Zero Power
Fast Critical Assemblies

by

P.E. Mc Grath and E.A. Fischer

Gesellschaft für Kernforschung mbH., Karlsruhe

A b s t r a c t

The methods utilized in the computer program KAPER (Karlsruhe Perturbation Evaluation Routine) are presented. The program is a multigroup cell code for the calculation of cross sections, fluxes, reaction rates, and small-sample reactivity worths in the plate geometry of zero power critical assemblies. The methods in the program are based on integral transport theory in the collision probability formulation. The resonance self-shielding of the cross sections in the multiregion cells are calculated with a formulation based on the f-factor concept. The program has the unique feature of treating local perturbations in the normal unit cell in which the local properties of the cell have been changed as a result of the experiments. Small-sample reactivity worths are found with perturbation theory in which the perturbed flux in the sample and environment is used.

Application of the program in the analysis of measurements performed in the zero power critical facility SNEAK at Karlsruhe is described. The measurements include reaction rates and small-sample reactivity worths.

1. März 1972

Zusammenfassung

Die Methoden, die in dem Rechenprogramm KAPER (Karlsruhe Perturbation Evaluation Routine) verwandt wurden, werden erläutert. Das Programm KAPER ist ein Vielgruppen-Zellprogramm zur Berechnung von Querschnitten, Flüssen, Reaktionsraten und den Materialwerten kleiner Proben in Plattengeometrie von kritischen Nulleistungsanordnungen. Die Methode in dem Programm basiert auf der Integral-Transporttheorie in der Stoßwahrscheinlichkeitsformulierung. Die Resonanz-Selbstabschirmung der Querschnitte in der Vielregionenzelle wird durch Verwendung des f-Faktorbegriffs berücksichtigt. Das Programm hat die einmalige Eigenschaft, lokale Störungen in einer Normalzelle zu behandeln, in der die lokalen Eigenheiten der Zelle infolge des Experiments verändert wurden. Die Materialwerte der kleinen Proben werden mit Hilfe der Störungstheorie berechnet, in die der gestörte Fluß von Probe und Umgebung eingeht.

Die Verwendung des Programms zur Analyse von Messungen an der kritischen Nulleistungsanordnung SNEAK in Karlsruhe wird beschrieben. Diese Messungen schließen Reaktionsraten und Materialwerte von kleinen Proben ein.

Table of Contents

Page

1. Introduction	1
2. Calculation of Heterogeneous Cross Sections and Fluxes	2
2.1 Basic equations	4
2.2 A consistent formalism for fast reactor cell calculations based on the f-factor concept	6
2.3 Approximations utilized	11
2.4 Leakage corrections	13
2.5 Heterogeneous flux and adjoint calculation in a periodic cell	16
2.6 Flux and adjoint calculation in a local perturbation of the periodic reactor cell	19
3. Heterogeneous Perturbation Calculation for Reactivity Worth Samples	24
3.1 Perturbations formulation	26
3.2 Normalization of perturbation equation	30
4. Numerical Results	31
4.1 Comparison of numerical results from heterogeneity calculations	31

	Page
4.2 Calculation of reaction rates in a perturbed environment	34
4.3 Analysis of reactivity worth measurements in SNEAK	35
5. Conclusions	37
Appendix: Methods used for the calculation of collision probabilities	39
References	42

1. Introduction

This report describes the methods utilized in a program, called KAPER (Karlsruhe Perturbation Evaluation Routine), for the calculation of heterogeneous cross sections, fluxes (real and adjoint), reaction rates, and reactivity worths in the heterogeneous plate structure of fast critical assemblies, e.g. the critical assembly SNEAK /1/ at Karlsruhe.

The theoretical foundation of the program is integral transport theory in the first-flight collision probability formulation. The cross sections for the cell of the assembly are prepared in a manner similar to that developed by Wintzer /2/ which accounts for the resonance self-shielding in multiregion cells. The fluxes are calculated by solving the integral transport theory equations in which leakage is accounted for through the neutron balance. The program has the capability of treating local disturbances in the periodic unit cell structure, which can be of importance for some reaction rate and reactivity worth calculations. To obtain the reactivity worths the cross sections and fluxes are used in a perturbation theory formulation of the integral transport theory equation. The perturbed flux in the sample and in its environment is obtained by solving the integral transport equations as a fixed source equation.

This report is divided into three main sections. The first deals with the calculation of the resonance self-shielded cross sections and fluxes in periodic unit cells. Also included is the calculation of fluxes in the special case in which a local disturbance has been introduced in the unit cell. The second section is devoted to the calculation of small-sample reactivity worths. Finally in the last section numerical results are given for the verification of the methods used in the program. In addition, results derived from the application of the KAPER program to the analysis of measurements performed in some SNEAK /1/ assemblies are also given.

2. Calculation of Heterogeneous Cross Sections and Fluxes

In the interpretation of nearly all experiments performed in the lattices of fast critical assemblies it has been found that heterogeneity effects are of importance and must be taken into account. This is frequently accomplished by utilizing equivalence theorems for the effective cross sections. However the usefulness of this procedure is restricted to very simple cells, for example cells of one fuel region and one moderator region.

Therefore a procedure was developed by Wintzer /2/ for the calculation of heterogeneity effects in periodic fast reactor cells in which there are no restrictions on the location of the resonance materials nor the division of the cell into regions. Wintzer's procedures lead to the development of the computer code ZERA at Karlsruhe. The methods employed by the code may be characterized as follows:

- a) Collision probability method,
- b) Concept of the self-shielding factor ('f-factor concept'),
- c) A method devised by Wintzer to calculate resonance self-shielding in complex multi-region cells,
- d) Solution of the integral Boltzmann equation in terms of the neutron source densities, and
- e) A method based on neutron balance considerations to account for leakage.

The ZERA code is used on a routine basis at Karlsruhe, and seems to give good results in most practical cases. However, the approximations used by ZERA are complex and may not be valid in cases

of extremely strong heterogeneity. An objective of this work was to modify and improve the procedures used in the ZERA code primarily in the application of the 'f-factor-concept' to heterogeneity calculations.

The concept of the composition-dependent self-shielding factor ('f-factor'), which was first introduced by Abagjan et al. /3/, is used in the standard 26-group calculations for fast reactors at Karlsruhe. The obvious limitation of this concept comes from the fact that it contains no information on the distribution of the resonances of one particular isotope within an energy group. Therefore, for very accurate calculations one has to resort to codes like RABBLE, developed at Argonne, or GENEX from Winfrith, which take account of the exact parameters of each particular resonance. These codes necessarily have to use an ultrafine energy group structure, and are, therefore, not suitable for routine calculations. On the other hand, the 'f-factor concept' is a fair approximation in most calculations for homogeneous media, and will certainly be used extensively in the future.

In this context, the question arises whether the 'f-factor concept' can be satisfactorily applied to heterogeneity calculations. The manner in which the concept is used in ZERA is not entirely consistent, because the reaction coefficients, which are calculated for each isotope separately /2/, depend rather strongly on the background cross section due to the other isotopes, so that some ambiguity is present.

In section 2.2 it is demonstrated that a consistent formalism which uses the f-factor concept for heterogeneous problems is possible in principle; however, it is far too complicated to be used in practical calculations. Therefore, an approximate method must be used anyway. The method suggested in this report is based on effective cross sections, which depend only weakly on the background cross section used. With these cross sections, one solves

the Boltzmann equation in terms of the fluxes, rather than the neutron source densities. The approximations used in this method are similar to those inherent in homogeneous calculations.

2.1 Basic Equations

The basic equations of the collision probability method will be briefly summarized here.

The integral energy dependent Boltzmann equation is in the case of isotropic scattering,

$$\Sigma_t(E, \bar{r}) \phi(E, \bar{r}) = \int d^3r' S(E, \bar{r}') p(\bar{r}' \rightarrow \bar{r}, E). \quad (2.1)$$

The nomenclature used is standard.

The first-flight collision probability p is given by

$$p(\bar{r}' \rightarrow \bar{r}, E) = \frac{\Sigma_t(E, \bar{r})}{4\pi} \frac{e^{-\tau(\bar{r}', \bar{r}, E)}}{|\bar{r}' - \bar{r}|^2} \quad (2.1a)$$

where τ is the optical path length between r' and r at energy E . The neutron source density $S(E, r)$ is composed of the fission source and the slowing down source in the following manner:

$$S(E, \bar{r}) = \int dE' \phi(E', \bar{r}) \left\{ \Sigma_s(E' \rightarrow E, \bar{r}) + \chi(E) \nu \Sigma_f(E', \bar{r}) \right\} \quad (2.2)$$

For practical calculations, one has to derive equations in the multigroup formalism from (2.1) and (2.2). The usual manner is to postulate the narrow resonance approximation and to observe that the source density $S(E,r)$ shows no resonance structure within this approximation. Then, the obvious procedure is to eliminate the flux $\phi(E,r)$ between Eqs. (2.1) and (2.2), and to write the equations in the multigroup form with the source density S as a variable

$$S^g(\vec{r}) = \sum_{g'} \int d^3r' S^{g'}(\vec{r}') \left[\left\langle \frac{\Sigma_{s^{g' \rightarrow g}}}{\Sigma_t}(\vec{r}) p(\vec{r}' \rightarrow \vec{r}, E) \right\rangle_{g'} \right. \\ \left. + \chi^g \left\langle \frac{\nu \Sigma_f^{g'}}{\Sigma_t}(\vec{r}) p(\vec{r}' \rightarrow \vec{r}, E) \right\rangle_{g'} \right] \quad (2.3)$$

where g is the index of the energy group, and the brackets $\langle \rangle$ indicate averages over energy.

The energy-averaged quantities

$$A_\alpha(\vec{r}', \vec{r}) = \left\langle \frac{\Sigma_\alpha}{\Sigma_t}(E, \vec{r}) p(\vec{r}' \rightarrow \vec{r}, E) \right\rangle \quad (2.4)$$

referred to as reaction coefficients for the reaction of type α by Wintzer /2/, are solved in the ZERA code.

There is, however, an alternative procedure which consists of eliminating the source densities S between Eqs. (2.1) and (2.2). The resulting flux equations are, in multigroup form,

$$\Sigma_t^g(\vec{r})\Phi^g(\vec{r}) = \int d^3r' \left\langle p(\vec{r}' \rightarrow \vec{r}, E) \right\rangle_g \sum_{g'} \left[\Sigma_s^{g' \rightarrow g}(\vec{r}') \right. \\ \left. + \chi^g \nu \Sigma_f^{g'}(\vec{r}') \right] \Phi^{g'}(\vec{r}') \quad (2.5)$$

where the effective cross sections $\Sigma_\alpha^g(\vec{r})$ are defined by

$$\Sigma_\alpha^g(\vec{r}) = \frac{\int d^3r' \left\langle \frac{\Sigma_\alpha(E, \vec{r}) p(\vec{r}' \rightarrow \vec{r}, E)}{\Sigma_t} \right\rangle_g S^g(\vec{r}')}{\int d^3r' \left\langle \frac{1}{\Sigma_t(E, \vec{r}) p(\vec{r}' \rightarrow \vec{r}, E)} \right\rangle_g S^g(\vec{r}')} \quad (2.6)$$

It must be emphasized that the systems of equations (2.3) and (2.5) are completely equivalent within the narrow resonance approximation, which is inherent in the f-factor concept anyway. At first sight, the system (2.5) seems to be unnecessarily complicated because the source densities appear in the definition (2.6) of the effective cross sections, and consequently must be calculated anyway. Thus, it appears, that the method used in ZERA should be preferred. However, it is shown that the cross sections (2.6) depend only weakly on the source densities. In fact, they can be calculated more accurately than the reaction coefficients (2.4), as is shown in Section 4.1. Therefore, the flux equations (2.5) and effective cross sections (2.6) are utilized in this work.

2.2 A consistent formalism for fast reactor cell calculations based on the f-factor concept

It will be shown that a consistent formalism based on the concept of the self-shielding factors is possible under the additional

hypothesis that the resonances of an isotope are randomly distributed within an energy group, and, therefore, the average of the product

$$\langle f(\sigma_1) g(\sigma_2) \rangle$$

over energy is simply the product of the averages

$$\langle f(\sigma_1) g(\sigma_2) \rangle = \langle f(\sigma_1(E)) \rangle \langle g(\sigma_2(E)) \rangle$$

where σ_1 and σ_2 are cross sections of different isotopes and f and g denote functions of σ_1 and σ_2 . This hypothesis is the only plausible one, as there is nothing known about the actual distribution of resonances.

The quantities which must be calculated in the collision probability method are the reaction coefficients defined by equation (2.4)

$$A_{\alpha mn} = \left\langle \frac{\Sigma_{\alpha n}}{\Sigma_{tn}}(E) p_{mn}(E) \right\rangle \quad (2.4a)$$

which in actuality are reaction probabilities. They are defined as the number of reactions of type α in region n due to a uniform unit source in region m . Once the $A_{\alpha mn}$ are known, the solution of the source equations is straight forward.

$A_{\alpha mn}$ may be defined as an integral over regions m and n .

To be specific, we write for an infinite slab lattice

$$A_{\alpha mn} = \frac{1}{X_m} \int_{X_m} dX' \int_{X_n} dX A_{\alpha}(X', X) \quad (2.7)$$

where

$$A_{\alpha}(X', X) = \left\langle \frac{\Sigma_{\alpha n}}{\Sigma_{tn}}(E) p(X' \rightarrow X, E) \right\rangle$$

The cross sections are assumed constant in each particular region.

In Eq. (2.7) X_m is the thickness of region m , and the integrals are over regions m and n . The probabilities $A_{\alpha}(X', X)$ are given by

$$A_{\alpha}(X', X) = \left\langle \frac{\Sigma_{\alpha n}(E)}{2} \int_1^{\infty} \frac{dt}{t} e^{-\tau(X', X, E)t} \right\rangle \quad (2.8)$$

where τ is the optical path length between X' and X

$$\tau(X', X, E) = \int_{X'}^X \Sigma_t(X'', E) dX''$$

Obviously, τ may be split into contributions of the isotopes present

$$\tau = \sum_v d_v(X', X) \sigma_{tv}(E)$$

where d_v is the number of nuclei of isotope v per cm^2 between X' and X . If N_{vn} is the atom density of isotope v in region n , one has

$$A_{\alpha}(X', X) = \frac{1}{2} \int_1^{\infty} \frac{dt}{t} \sum_v N_{vn} \left\langle \sigma_{v\alpha}(E) \exp(-t \sum_{v', v''} d_{v', v''}(X', X) \sigma_{tv', v''}(E)) \right\rangle \quad (2.9)$$

By hypothesis, the product over isotopes in the brackets can be written as follows

$$\begin{aligned}
 A_{\alpha}(X', X) &= \frac{1}{2} \int_1^{\infty} \frac{dt}{t} \sum_v N_{vn} \left\langle \sigma_{v\alpha}(E) e^{-td_v \sigma_{tv}} \right\rangle \prod_{v' \neq v} \left\langle e^{-td_{v'} \sigma_{tv'}} \right\rangle \\
 &= \frac{1}{2} \int_1^{\infty} \frac{dt}{t} \sum_v N_{vn} S_{\alpha v}(td_v) \prod_{v' \neq v} T_{v'}(td_{v'})
 \end{aligned}
 \tag{2.10}$$

where the $T_{v'}$ are transmission probabilities, and S_{α} is an effective microscopic cross section of isotope v , defined by

$$S_{\alpha}(y) = \left\langle \frac{\sigma_{\alpha}(E)}{\sigma_{\alpha}(E) + y} \right\rangle$$

Leaving out the subscript v , we observe from the relation

$$R_{\alpha}(\sigma_0) = \left\langle \frac{\sigma_{\alpha}}{\sigma_{\alpha} + \sigma_0} \right\rangle = \int_0^{\infty} \left\langle \sigma_{\alpha} e^{-y\sigma_{\alpha}} \right\rangle e^{-y\sigma_0} dy = L \left[S_{\alpha} \right]
 \tag{2.11}$$

that S_{α} is the inverse Laplace transform of R_{α} , which is related through the equation

$$R_{\alpha}(\sigma_0) = \frac{\tilde{\sigma}_{\alpha}(\sigma_0)}{\tilde{\sigma}_{\alpha}(\sigma_0) + \sigma_0}$$

to the self-shielded cross sections $\tilde{\sigma}_{\alpha}$, i.e. to the self-shielding factors. The transmission probability T is given by

$$T(y) = \left\langle e^{-y\sigma_t} \right\rangle$$

It is connected to R_t through the equation

$$R_t(\sigma_0) = \left\langle \frac{\sigma_t}{\sigma_t + \sigma_0} \right\rangle = 1 - \sigma_0 L [T] \quad (2.12)$$

which follows immediately from

$$S_t = -dT/dy$$

Thus, we have shown that the reaction coefficients A_{α} in a slab lattice can be expressed rigorously, via the Eqs. (2.7), (2.8), (2.11), (2.12), through the function $R_\alpha(\sigma_0)$, which is immediately given by the self-shielding factors. Oosterkamp /4/ has carried the argument one step further and observed that, for a given isotope,

$$S_\alpha(y) = \iint \sigma_\alpha e^{-y\sigma_t} w(\sigma_\alpha, \sigma_t) d\sigma_\alpha d\sigma_t$$

where $w(\sigma_\alpha, \sigma_t) d\sigma_\alpha d\sigma_t$, is the probability that the cross section for reaction α and the total cross section take on the pair of values σ_α, σ_t in an energy group which contains resonances. Thus, $S_\alpha(y)$ is the Laplace transform of the probability distribution

$$W_\alpha(\sigma_t) = \int \sigma_\alpha w(\sigma_\alpha, \sigma_t) d\sigma_\alpha \quad (2.13)$$

and one could work out an analysis which is based on tabulated functions of the type (2.13). However, if one notes that a lattice may typically contain a dozen isotopes, a simple count of the integrations which have to be performed starting from Eq. (2.10), shows that these equations are definitely not feasible for use

in routine calculations. Therefore, one has to resort to approximations which drastically reduce the complexity of the equations.

It should be emphasized that it is not of interest to have a heterogeneity code based on the f-factor concept which requires long running times, and thus cannot be used in routine calculations. At the expense of long computer time, one can run a RABBLE calculation, and get answers which are free from the restrictions of the f-factor concept. However, it may also be reasonable to integrate Eqs. (2.7) to (2.10) in a few simple cases in order to check the validity of the approximate methods.

2.3 Approximations Utilized

In the original ZERA code, the reaction coefficients defined by (2.4) are constructed from the contributions of the single isotopes, labeled v

where

$$A_{\alpha mn} = \sum_v A_{\alpha v mn}, \quad A_{\alpha v mn} = \left\langle \frac{\sum \sigma_{\alpha v n}}{\sum t_n} P_{mn} \right\rangle$$

This quantity is approximated by

$$A_{\alpha v mn} = \left\langle \frac{\sigma_{\alpha v}}{\sigma_{tv} + \sigma_{on}} P_{mn} (\sigma_{tv}, \sigma_o) \right\rangle \quad (2.14)$$

where σ_{tv} = total effective cross section of isotope v
 and σ_{on} = sum of total effective cross section of all isotopes except v in region n , normalized to one atom of v .

The background cross sections σ_{on} and σ_o are assumed constant in energy. This means that they have to be averaged over resonances in a way that is not well defined. However, these quantities are fairly sensitive to the choice of the

background cross sections, especially in strongly heterogeneous lattices. It is for this reason that the KAPER program uses, instead, the effective cross sections (2.6), which are for one particular isotope:

$$\tilde{\sigma}_{avn} = \frac{\sum_m \left\langle \frac{\sigma_{av}}{\sigma_{tv} + \sigma_{on}} p_{mn} \right\rangle S_m}{\sum_m \left\langle \frac{1}{\sigma_{tv} + \sigma_{on}} p_{mn} \right\rangle S_m} \quad (2.15)$$

The approximation (2.15) is certainly good since, as will be shown, the effective cross sections are insensitive to the background cross section. This was observed, for example, in /5/ for the homogeneous case. It is demonstrated in Section 4.1 that this is also true for the heterogeneous case. It should be noted that the reaction coefficients (2.14) are needed to calculate (2.15).

The group averaged collision probabilities $\left\langle P_{mn}(E) \right\rangle_g$ must be calculated. The averaging process over energy defines a certain manner of self-shielding, which, however, is rather complicated. Therefore, at this point, the assumption is made, that the collision probabilities may be calculated approximately with the effective cross sections defined by Eq. (2.15).

Obviously, this approximation is the equivalent in the heterogeneous case to the approximations used in homogeneous calculations, and in fact the expression (2.15) is completely analogous to the expression for the self-shielded cross sections in the homogeneous case. Thus, though we were not able to derive the use of the cross sections defined by (2.15) to calculate the collision probabilities from mathematical principles, we believe that this method is as accurate as most other standard calculations within the Karlsruhe program system.

In the KAPER code, the source densities S_m , which appear in Eq. (2.15), are first approximated by the fully self-shielded total cross sections

$$S_m = \sum_v N_{vm} \sigma_{tv} (\sigma_o = 0) \quad (2.16)$$

An iteration on the source densities can be carried out if required. The results that are quoted in Section 4 show that iteration leads only to small changes in the effective cross sections, so that the first approximation (2.16) is good enough in most cases.

2.4 Leakage Corrections

To discuss the formalism used to account for leakage in the code, let us assume a homogeneous medium and seek the fundamental mode solution of Eqs. (2.1) and (2.2) in the form

$$S(E, \vec{r}) = S(E) e^{i \vec{B} \cdot \vec{r}}$$

$$\phi(E, \vec{r}) = \phi(E) e^{i \vec{B} \cdot \vec{r}}$$

In this case, we have

$$p(\vec{r}' \rightarrow \vec{r}, E) = \frac{\Sigma_t}{4\pi} \frac{e^{-\Sigma_t |\vec{r}' - \vec{r}|}}{|\vec{r}' - \vec{r}|^2}$$

and, if the variable $\vec{\rho} = \vec{r}' - \vec{r}$ is introduced, the right side of Eq. (2.1) becomes

$$\int d^3\rho S(E) \frac{\Sigma_t}{4\pi} \frac{e^{-\Sigma_t \rho}}{\rho^2} \exp \left[i \vec{B} \cdot \vec{r} + i \vec{B} \cdot \vec{\rho} \right]$$

The above integration can be carried out, resulting in, for Eq. (2.1),

$$\Sigma_t(E)\phi(E) = S(E) \frac{\Sigma_t(E)}{B} \operatorname{arctg} \frac{B}{\Sigma_t(E)} \quad (2.17)$$

Averaging the equation over energy group g leads to

$$\Sigma_t^g \phi^g = S^g \left\langle \frac{\Sigma_t}{B} \operatorname{arctg} \frac{B}{\Sigma_t} \right\rangle_g$$

It is now assumed that the flux curvature B is weak, so that $B/\Sigma_t \ll 1$ over the entire range of E , the energy. Then one has, to first order in B^2/Σ_t^2 ,

$$\operatorname{arctg} \frac{B}{\Sigma_t} = \frac{B}{\Sigma_t} - \frac{1}{3} \left(\frac{B}{\Sigma_t} \right)^3$$

and, therefore, Eq. (2.17) may be written

$$\Sigma_t^g \phi^g = S^g \left(1 - \frac{B^2}{3} \left\langle \frac{1}{\Sigma_t^2} \right\rangle_g \right)$$

If we replace

$$\frac{1}{3} \frac{\left\langle \frac{1}{\Sigma_t^2} \right\rangle_g}{\left\langle \frac{1}{\Sigma_t} \right\rangle_g}$$

by D^g in the spirit of the transport approximation, we have to first order in B^2/Σ_t^2

$$S^g = (\bar{\Sigma}_t^g + \bar{D}^g B^2) \phi^g \quad (2.18)$$

This equation has a simple physical interpretation: The source neutrons in a certain volume make either a collision in the volume, or else they leak out without a collision.

We now require that Eq. (2.18) should be valid, in the case of a cell calculation, for the cell-averaged rates. Thus, the cell-integrated equation, Eq. (2.1), for the infinite lattice

$$V_{\text{cell}} \bar{\Sigma}_t \bar{\phi} = \int_{\text{cell}} d^3r S(\vec{r})$$

is replaced, for the finite lattice, by

$$V_{\text{cell}} (\bar{\Sigma}_t + \bar{D}B^2) \bar{\phi} = \int_{\text{cell}} d^3r S(\vec{r}) \quad (2.19)$$

to account for the leakage. This equation is in line with the method used by Benoist /6/, so that D can be calculated by the methods described in /6/. From Eq. (2.1), it is obvious that (2.19) is equivalent to scaling the collision probabilities in the following manner:

$$P_{mn} \longrightarrow \frac{\bar{\Sigma}_t}{\bar{\Sigma}_t + \bar{D}B^2} P_{mn}$$

The method just outlined is equivalent with the one derived by Wintzer /2/ from neutron balance considerations.

2.5 Heterogeneous flux and adjoint calculation in a periodic cell

The heterogeneous flux distribution within a unit cell is calculated by solving numerically the following equation:

$$V_m \Sigma_{t_m}^g \phi_m^g = \sum_{nk} V_n \Sigma_n^{k \rightarrow g} \phi_n^k P_{nm}^g \quad (2.20)$$

where n and m are geometrical region indices,

g and k are energy group indices,

V_n = volume of the n^{th} region,

$$\Sigma_n^{k \rightarrow g} = \Sigma_{s_n}^{k \rightarrow g} + \lambda v \Sigma_f^n^k \chi_n^g,$$

λ = eigenvalue = $1/k_{\infty}$ (no leakage)

= $1/k_{\text{eff}}$ (leakage introduced),

and P_{nm}^g = probability a neutron originating in group g and region n of suffering its first collision in region m . (This probability includes the contribution of those neutrons from region n that leak from the cell, without suffering a collision, and collide in identical regions m of the surrounding cells).

The Eq. (2.20) is obtained from Eq. (2.5) by integrating over the regions of the cell and assuming the flat-flux approxima-

tion. Since one can divide the platelets that constitute the cell into as many regions as desired this approximation is of little consequence.

Because the P_{nm}^g in Eq. (2.20), and all other equations having collision probabilities, are calculated exactly (see appendix) there is no assumption made about the flux, or neutron current, at the boundary of the cell.

The macroscopic cross sections in Eq. (2.20) are defined from the microscopic cross section as given by Eq. (2.15).

Eq. (2.20) can be thought of as the microscopic integral transport theory equation since by definition of the collision probabilities the unit cell has been isolated from the remaining portion of the core. This same equation could be used to obtain the eigenvalue and flux for a core and blanket configuration simply by redefining the collision probabilities to include all regions of the core and blanket. In this case the equation can be referred to as the macroscopic integral transport theory equation.

The adjoint flux is obtained from solution of the equation adjoint to Eq. (2.20) above. This equation is

$$\sum_t^g \phi_m^{+g} = \sum_n \sum_k \Sigma_n^g \rightarrow k \phi_n^{+k} P_{mn}^k \quad (2.21)$$

where the constants are the same as defined in Eq. (2.20).

These two equations, Eq. (2.20) and (2.21), are solved by the power iteration method. Convergence is assumed when the following condition is fulfilled in an outer iteration,

$$\left| 1 - \frac{\alpha^{(i-1)}{}^2}{\alpha^{(i)} \alpha^{(i-2)}} \right| \leq \epsilon \quad (2.22)$$

where $\alpha^{(i)}$ is the total cell fission source in Eq. (2.20) for outer iteration number i ,

$$\alpha^{(i)} = \sum_n \sum_k v_n v_{\Sigma f_n}^k \phi_n^k \quad (2.23)$$

or, for the adjoint equation,

$\alpha^{(i)}$ is the total cell importance source in Eq. (2.21) for outer iteration number i ,

$$\alpha^{(i)} = \sum_n \sum_m \sum_k X_m^k \phi_m^{k+1} P_{nm}^k \quad (2.24)$$

The three point convergence formula, Eq. (2.22), is slightly more stringent than the normally used two point formula for a given convergence parameter ϵ .

Within an outer iteration a convergence criterion is utilized for the fluxes. The fluxes in an inner iteration are considered converged when for energy region m and group g the fluxes satisfy the following condition:

$$\left| 1 - \frac{\phi_m^g(j)}{\phi_m^g(j-1)} \right| \leq \delta$$

where j is the inner iteration number and δ is the convergence parameter.

Normally convergence is achieved quite rapidly with this procedure, for example, in less than 5 outer iterations to a conver-

gence of 10^{-5} . The flux is then normalized to one fission neutron in the unit cell and the adjoint to a total importance of one for all fission neutrons.

The leakage from the reactor in the microscopic equations, Eqs. (2.20) and (2.21), is accounted for by multiplying the collision probabilities P_{nm}^g by the non-leakage probability L^g , as defined in section 2.4,

$$L^g = \frac{\Sigma_t^g}{\Sigma_t^g + D^g B^2}$$

where Σ_t^g and D^g are, respectively, the cell flux-averaged total cross section and the cell flux-averaged diffusion coefficient. Since the fluxes needed to calculate Σ_t^g and D^g are not known a priori the calculation of the non-leakage probabilities is included in the outer iteration procedure of the solution of Eq. (2.20). With the fluxes calculated in a given iteration the non-leakage probabilities are calculated. Then all collision probabilities in Eq. (2.20) are multiplied with these probabilities before another series of inner iterations are initiated.

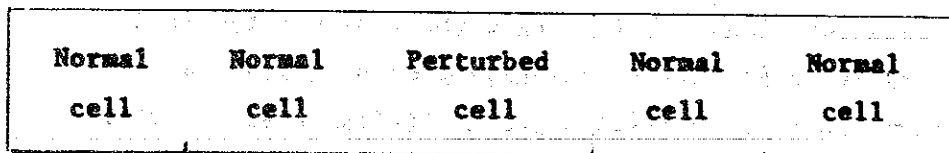
In the solution of Eq. (2.21) the collision probabilities are also multiplied by the non-leakage probability as calculated from the flux equation.

2.6 Flux and Adjoint Calculation in a Local Perturbation of the Periodic Reactor Cell

In many incidences measurements in a fast critical assembly involve a disturbance of the repeating unit cell. The following cases can easily be envisioned:

- a) A cell, or a portion of a cell, is removed for the insertion of a channel in which reaction rates are to be measured.
- b) A low density plate of inert material may be inserted between two plates of the cell in the position in which a sample is to be placed for reactivity measurements.
- c) The immediate environment of a reactivity worth sample may be altered to study the effect of the environment on the sample worth.

For clarity in the following discussion we will define the normal cell as that which constitutes the normal unit cell of the core. The perturbed cell is defined as a cell which contains a local perturbation in the normal unit cell. Therefore we may picture the situation as shown below in which a perturbed cell is surrounded by an infinite



repetition of normal cells. These cells may be composed of many plates of different materials.

One further point must be made clear concerning what constitutes a perturbed cell. Because of the manner in which the program KAPER works, and the assumptions utilized in the derivation of the following equations, a perturbed cell must consist of the region of local perturbation plus several normal unit cells on each side of the perturbed region. The exact number of normal unit cells depends on the magnitude of the perturbation introduced and the mean free path length of a neutron in the normal unit cell. Normally a perturbed cell of approximately two mean free paths in width is more than sufficient. The reason for

this restriction on the size of the perturbed cell is a result of the methods, as explained below, utilized in the KAPER program. The flux spectrum at the boundary of the perturbed cell must reach approximately its equilibrium value.

In these cases to solve for the appropriate flux and adjoint distribution in the perturbed cell it is assumed that the change in the reactor core (introduction of the perturbed cell) is sufficiently small as to not affect the criticality constant of the reactor nor the spectrum a few mean free paths from the perturbed cell position. With the above assumptions the flux and adjoint distribution in the perturbed cell can be obtained by solving the fixed source equations. The source is the first-flight leakage (uncollided neutrons) from the surrounding normal cells, or in the case of the adjoint equation, the importance a neutron from the perturbed cell has upon escaping from the perturbed cell.

To distinguish quantities which are a function of the normal cell from those of the perturbed cell we will write the quantities with an N or P in brackets for the normal and perturbed cell respectively. For example the region m , group g flux is $\phi_m^g(N)$ in the normal cell and $\phi_m^g(P)$ in the perturbed cell. With this notation in mind the fixed source equations may be written in the following manner:

A) Flux equation

$$V_m(P) \Sigma_{t_m}^g(P) \phi_m^g(P) = \sum_n \sum_k V_n(P) \Sigma_n^{k \rightarrow g}(P) \phi_n^k(P) P_{nm}^{+g}(P) + S_m^g(P) \quad (2.25)$$

where the region indices n and m are for regions only within the perturbed cell,

P_{nm}^{+g} = first-flight collision probability of a neutron in group g originating in region n to suffer a collision in region m of the perturbed cell.

and S_m^g = total external neutron source in group g and region m from the surrounding normal cells.

The remaining constants are the same as defined in Eq. (2.20) except that they are defined only for the perturbed cell. The cross sections are calculated as described in the previous sections, namely with Eq. (2.15), except that now the collision probabilities in, for example, Eq. (2.15) are defined for the perturbed cell surrounded by an infinite repetition of normal cells.

One can derive Eq. (2.25) quite easily by equating the total collision density in a group g and region m of the perturbed cell to the total collision source from other regions of the perturbed cell and from the surrounding normal cells (S_m^g).

The external source in Eq. (2.25) is found from the definition

$$S_m^g(P) = \sum_n \sum_k V_n(N) \Sigma_n^{k \rightarrow g}(N) \phi_n^k(N) \epsilon_{nm}^g(N) \quad (2.26)$$

where the region summation is over the regions in the normal cell and

$\epsilon_{nm}^g(N)$ = probability that a neutron from any region n of the normal cells suffers a collision in region m of the perturbed cell.

When the leakage from the reactor is accounted for in the solution of Eq. (2.25) the same non-leakage probability L^g as calculated for the normal cell is used in Eqs. (2.25) and (2.26) above. In this case the probabilities $P_{nm}^{+g}(P)$ and $\epsilon_{nm}^g(N)$ are multiplied by L^g . This approximation is

reasonable since the leakage from the core is determined by the mean free path in the core material (normal cell) and is influenced little by a change in one or two cells of the core.

B) Adjoint equation

$$\phi_m^{+g}(P) = \sum_n \sum_k \frac{\Sigma_m^{g \rightarrow k}(P)}{\Sigma_t^g(P)} P_{mn}^{+k}(P) \phi_n^{+k}(P) + S_m^{+g}(P) \quad (2.27)$$

The constants in this equation are the same as defined for Eq. (2.25) except for $S_m^{+g}(P)$, the fixed adjoint source. This is defined in the following manner:

$$S_m^{+g}(P) = \sum_k \frac{\Sigma_m^{g \rightarrow k}(P)}{\Sigma_t^g(P)} \sum_n \epsilon_{mn}^{+k}(P) \phi_n^{+k}(N) \quad (2.28)$$

where the region summation n is over the regions of the normal cell and

$\epsilon_{mn}^{+k}(P)$ = probability that a neutron from region m of the perturbed cell suffers a collision in any region n of the normal cells.

One can see that $S_m^{+g}(P)$ is the total importance of those neutrons in group g and region m of the perturbed cell which leak from the cell and suffer a collision in the surrounding normal cells. Therefore Eq. (2.27) represents a balance of importance for the colliding neutrons. It can easily be derived from this principle.

Again if leakage from the reactor core is accounted for the probabilities $P_{mn}^{+g}(P)$ in Eq. (2.27), and $\epsilon_{mn}^{+k}(P)$ in Eq. (2.28), are multiplied by the non-leakage probability L of each group.

The solutions of Eqs. (2.25) and (2.27) are obtained in the same manner as those from Eqs. (2.20) and (2.21), by the power iteration method with the convergence criteria of Eq. (2.22). The initial estimate of the flux spectra is chosen to be that of the normal cell. However in this case no renormalization of the fluxes is used since it is determined by the magnitude of the sources $S_m^g(P)$ and $S_m^{+g}(P)$ in the respective equations.

3. Heterogeneous Perturbation Calculation for Reactivity Worth Samples

Small-sample reactivity measurements performed in fast critical assemblies are integral experiments which can be performed with high precision. Representative of these experiments is the material substitution measurement. In this measurement a sample of material under study is inserted into the assembly and the resulting reactivity of the assembly, relative to a reference, is measured.

However the calculation of the reactivity worth of small-samples in the heterogeneous environment of the fast critical is generally a difficult problem. Normally the self-shielding within the sample, and the heterogeneity of the sample environment, are neglected. That is, as performed at Karlsruhe, the worths are calculated with a first-order multigroup homogeneous diffusion theory formulation of perturbation theory. The cross sections, for the homogeneous core material and for a composition containing core material plus a small amount of the sample material, are obtained utilizing the concept of composition - dependent resonance self-shielding factors, as described by Abagyan et al./3/. The reactivity worth of the sample is then calculated as the difference between the core material and the core material with the small amount of sample material.

In hard spectrum cores (long mean free paths) with small simple unit cells and thin samples, this approach is generally adequate since the self-shielding factors involved are those of the core material. When these conditions are not present the above procedure can give results several percent in error. Since small sample reactivity worth studies in SNEAK and other fast critical assemblies have been performed in relatively soft spectrum cores with complex cell structures it seems imperative to refine our calculational methods for the analysis of this particular type of experiment.

Over the past few years there have been many improvements in the calculation of heterogeneous reactivity worths. The work of several authors /7,8/ lead to corrections for flux depression in an absorber when the cross sections are smooth. Fischer /9/ developed a program to correctly account for the self-shielding in the sample, thereby describing the flux depression in an absorber and the dependence of the resonance self-shielding on the geometry of the sample. However in this work the sample environment is treated as homogeneous. Oosterkamp /4/ treats in his work the heterogeneous environment of the sample as well as the self-shielding of the sample.

The objective of the work described in this report was to develop a program similar to that of Oosterkamps but more flexible in utility, with simpler methods (thereby easing the numerical problems), and with better defined cross sections for the sample.

In many cases the measurement of the reactivity worth of a sample necessitates a perturbation of the normal cell structure of the assembly. For example a low density plate of inert material may be inserted between two plates of the cell in the position in which a sample is to be placed for

reactivity measurements. In some incidences it may be necessary to account for this perturbation when calculating the reactivity worths. Therefore a program flexible enough to account for this effect is desirable.

3.1 Perturbation Formulation

For the calculation of heterogeneous reactivity worths perturbation theory is used. Perturbation theory offers an advantage for the calculation of small changes in a system; this being that the change in the system is expressed directly in equation form rather than being the difference of two nearly equal quantities as one would get by calculating the eigenvalue separately for the perturbed and unperturbed systems.

Therefore the heterogeneous fluxes and cross sections, obtained as described in the previous sections, are used in a perturbation theory formulation of the integral transport theory equation to obtain reactivity worths of small changes introduced into the reactor core. It would be possible to produce homogeneous cross sections by averaging the heterogeneous cross sections with the heterogeneous fluxes for use in, for example, a one dimensional diffusion theory perturbation theory program. This procedure was not utilized for the primary reason that the first order perturbation theory formulation based on integral transport theory, Eq. (2.1), results in a higher order results /10/ than that of a formulation based on diffusion theory. This is related to the fact that the perturbation of the operator in integral transport theory is not linear in the cross section perturbation but contains terms of higher order. These higher order terms are a result of the collision probabilities in the perturbation operator.

However since the flux depression, or peaking, in the sample can be as important as the self-shielding of the sample cross sections

the exact form of the perturbation equation is utilized in the KAPER program rather than a first-order form as is commonly employed in perturbation programs. Therefore formulating the perturbation equation with the macroscopic integral transport theory flux equation (representing the perturbed state) and the adjoint equation (representing the unperturbed state) one obtains

$$\rho = \frac{1}{D\rho} \left[\sum_{g,m} V_m \phi_m^g \right] \left[-\delta \Sigma_{t,m}^g \phi_m^{+g} + \sum_{k,n} \delta (\Sigma_m^{g \rightarrow k} P_{mn}^k) \phi_n^{+k} \right] \quad (3.1)$$

where $\Sigma_m^{g \rightarrow k} = \Sigma_{S,m}^{g \rightarrow k} + \lambda v \Sigma_{f,m}^g \chi^k$, and the region index summations are over all regions, in the perturbed cell and the normal cell, where the perturbation operator $\delta (\Sigma_m^{g \rightarrow k} P_{mn}^k)$ is non-zero. The denominator of Eq. (3.1) is

$$D\rho = \lambda \sum_{g,m} V_m v \Sigma_{f,m}^g \phi_m^g \sum_{k,n} \chi^k \phi_n^{+k} P_{mn}^k$$

The perturbation operator, in general terms δN , is defined as $(N' - N)$ where the primed quantity denotes that defined for the perturbed state and that without the prime for the unperturbed state.

From experience it was found that the two terms in Eq. (3.1) are generally of the same order of magnitude with the difference being two or three orders of magnitude smaller than the individual terms. This is undesirable from a numerical point of view. Therefore rather than use Eq. (3.1) directly we can rewrite it in a different form.

Let us write the perturbation operator as the following:

$$\delta(\Sigma_m^{g-k} P_{mn}^k) = \delta\Sigma_m^{g-k} P_{mn}^k + \delta P_{mn}^k (\Sigma_m^{g-k})$$

In addition we may also use the relation between the source importance function ψ_m^{+k} and the colliding neutron importance function ϕ_m^{+k} (the adjoint flux as calculated in Section 2.5 and 2.6).

$$\psi_m^{+k} = \sum_n P_{mn}^k \phi_n^{+k}$$

Introducing these relations into Eq. (3.1) we can write the results as, after some rearranging,

$$\rho = 1/D_0 \sum_g \sum_m V_m \phi_m^g \left[-\delta\Sigma_a^g \phi_m^{+g} + \sum_k \delta\Sigma_a^{g \rightarrow k} (\psi_m^{+k} - \phi_m^{+g}) \right] \tag{3.2}$$

$$+ \lambda \delta(v\Sigma_f^g) \sum_k \chi_m^k \psi_m^{+k} + \sum_k \delta P_{mn}^k (\Sigma_m^{g \rightarrow k} + \lambda v \Sigma_f^g \chi_m^k) \phi_n^{+k} \left. \right]$$

where Σ_a^g = total absorption cross section in region m and energy group g.

This equation has a form that renders itself to easy physical interpretation. A source neutron, from a fission or scattering reaction, is weighted by the source importance function while a colliding neutron is weighted by the colliding neutron importance function. The last term of Eq. (3.2) accounts for diffusion effects.

However the form utilized in the KAPER program is slightly different than Eq. (3.2). We can rearrange the equation to

obtain the following results

$$\begin{aligned}
 0 = & \frac{1}{D_0} \sum_g \sum_m v_m \phi_m^g \left[-\delta \Sigma_a^g \psi_m^{+g} + \sum_k \delta \Sigma_s^{g-k} (\psi_m^{+k} - \psi_m^{+g}) \right. \\
 & + \lambda \delta (v \Sigma_f^g) \sum_k \chi_k^k \psi_m^{+k} + \delta \Sigma_t^g (\psi_m^{+g} - \phi_m^{+g}) \\
 & \left. + \sum_k \sum_n \delta P_{mn}^k (\Sigma_s^{g-k} + \lambda v \Sigma_f^g \chi_n^k) \phi_n^{+k} \right]
 \end{aligned} \tag{3.3}$$

The only advantage to Eq. (3.3) is that the first three terms can be identified as the normal absorption, scattering, and fission perturbation terms.

The perturbed flux in Eq. (3.3) is obtained with the procedure explained in Section 2.6. In this case the disturbance in the unit cell is the sample. By utilizing Eq. (2.25) to find the flux in and around the sample one accounts also for the perturbation, due to the sample, in the sample environment.

It must be remembered that the derivation of Eq. (3.3) is based on the macroscopic integral transport equations, therefore it is assumed that we have an infinite plate geometry medium which consists of the perturbed cell surrounded by an infinite number of normal cells as shown in a figure on page 20 in Section 2.6. When the region summations are over the perturbed cell, the flux and adjoint from the solution of Eqs. (2.25) and (2.27) are used, and for the normal cells the flux and adjoint are from the solution of Eqs. (2.20) and (2.21). The perturbed cross sections are found in the cross section phase portion of the KAPER program with the sample inserted in the

perturbed cell. For cores which have a significant flux curvature within a few mean free paths from the perturbed cell an energy group dependent cosine curve is superimposed upon the flux and adjoint distribution in space. This curve is calculated with

$$f^g(x) = \cos(B^g x)$$

where B^g is the square root of the group g Buckling and x is the distance from the geometrical center of the perturbed cell. Therefore we have then quasi-one dimensional fluxes with the heterogeneous fine structure superimposed.

3.2 Normalization of Perturbation Equation

Since the calculational procedure explained above is a zero dimensional, at best a quasi-one dimensional calculation, the denominator of Eq. (3.3) can not be calculated correctly for the actual reactor core and blanket. The calculation of the denominator, or normalization integral as it is commonly called, is best done with a multi-dimensional flux program, i.e. two-dimensional diffusion theory program DIXY of Karlsruhe. Therefore the procedure selected for the calculation of the denominator is as follows:

$$D_p = F(o) D_{NOR}$$

where

$$D_{NOR} = \frac{\lambda \sum_m \sum_n V_m \nu \Sigma_f^g \sum_k \sum_n \chi_n^{k+1} P_{mn}^k}{\sum_n V_n} \quad (3.4)$$

$$\text{and } F(o) = \frac{\int d\vec{r} \sum_g v \Sigma_f^g(\vec{r}) \psi(\vec{r}) \sum_k \chi^k \psi(\vec{r})}{\sum_g v \Sigma_f^g(o) \sum_k \chi^k \psi(o)}$$

In these equations it is assumed that the effect of the sample in the calculation of the normalization integral is negligible. Therefore the perturbed fission source is replaced by its unperturbed value. For small sample reactivity worths, for which this program is designed to handle, this approximation is quite valid.

The factor D_{NOR} is calculated for a normal cell. $F(o)$ is the normalization integral normalized by the neutron and importance source at the center of the reactor. The integration in $F(o)$ is over the entire reactor, core and blanket. The factor is obtained in an independent calculation, such as a two dimensional diffusion calculation, and is used as input data to the KAPER program for Eq. (3.3).

4. Numerical Results

In the following section a number of test calculations are given as verification of the methods utilized in the KAPER program. Following this the results derived from the application of the KAPER program on the analysis of measurements performed in some SNEAK assemblies are given.

4.1 Comparison of Numerical Results from Heterogeneity Calculations

In a first series of calculations with KAPER and the ZERA program /2/, k_{∞} was calculated for a cell similar to SNEAK-5C /11/;

this was a null-reactivity assembly with a soft spectrum and strong heterogeneity effects, which contained mainly mixed oxide and graphite. The calculations used 9 regions. In order to simplify the calculations, the less important isotopes were left out. The data used are given in Table Ia and Ib.

Tables II shows the k_{∞} values obtained for cells of different thickness. The following comments can be made:

- a) As expected from the theory, all results for the quasi-homogeneous case agree well. This indicates that no programming errors are involved.
- b) The two codes, ZERA and KAPER, using the same approximation for the collision probabilities, give δk values which differ by 0.6% δk for the full cell, and less than that for the smaller cells. Thus, the standard ZERA code may be used unless large heterogeneities are involved.
- c) The k_{∞} values before iteration on the source densities are given in brackets. The figures indicate that the changes due to the iteration are by one order of magnitude smaller than the difference in values given by the two codes. Therefore the iteration is necessary only in cases of large heterogeneity.

The dependence of the heterogeneity effect on the background cross section is demonstrated in Table III. The standard calculation uses background cross sections of U^{238} in the resonance groups equal to the potential cross section, which is $\sigma_p = 10.6$ barns. For comparison with ZERA calculations by Kiefhaber /12/, the background cross section was set equal to the total unshielded cross section σ_t in a second calcu-

lation. Whereas the δk obtained by Kiefhaber with ZERA (Table III) depends strongly on the background cross section, this dependence is very weak in the KAPER results. In fact, the KAPER k_{HET} depends on background cross section in much the same way as k_{HOM} , which is additional evidence for the conclusion that the approximations in the KAPER program are similar to the approximations in homogeneous calculations. Furthermore, as the resonances of U^{238} are strongly self-shielded, one would expect better results from ZERA by using σ_{p8} rather than σ_{t8} as a background cross section. This expectation is borne out by the results shown in Table II, where the ZERA δk is fairly close to the true KAPER δk .

The same KAPER calculations with σ_{p8} and σ_{t8} were used to obtain the dependence of the self-shielded cross section of Pu^{239} on the background. The results are shown in Table IV. Though the change in background cross section is very large, and σ_{t8} is certainly an extreme overestimate, the changes in the self-shielded cross sections are small, except for group 18. Thus, it is demonstrated that the cross sections defined by Eq. (2.15) are insensitive to the background cross sections.

For a second test case SNEAK-3A-2 /13/ was considered, which has been thoroughly studied, including bunching effects. For this high leakage core, the KAPER program gives again smaller δk 's than ZERA. The results are shown in Table V. Note that the δk is not linear; rather, in the bunched cases, the negative leakage increases stronger than the positive effects, so that the δk becomes even smaller. The small difference in the δk values for the homogeneous case from the two programs is probably due to different numerical procedures.

4.2 Calculation of Reaction Rates in a Perturbed Environment

In the hard spectrum core of SNEAK-7B /16/ studies were made on the effect of structural materials (stainless steel and aluminium) on spectral indices measured with foils. The core of SNEAK-7B consisted of a simple unit cell of one mixed oxide platelet (uranium and plutonium) and one uranium oxide platelet. For the measurements uranium foils were placed between the normal platelets of the cell to serve as reference. Additional foils were placed between stainless steel platelets, and aluminium platelets, of two thicknesses. This arrangement is illustrated in Fig. 1. The addition of the stainless steel, and aluminium represents a local perturbation in the normal repeating unit cell.

The methods described in Section 2.6 of this report were used to obtain the flux, and therefore the reaction rates, within these locally introduced perturbations in the normal unit cell. For the calculation a perturbed cell (as defined in Section 2.6) was selected to be the perturbation plus four normal unit cells on each side of the perturbation. The results of these calculations are shown in Fig. 2 and 3 for the MOXTOT cross section set of Karlsruhe. They are given as the percent change in the spectral indices σ_{c8}/σ_{f5} and σ_{f8}/σ_{f5} , respectively, with respect to the reference measurement (without additional structural material). While the agreement of the calculated and measured results does depend on the cross sections of the structural material, in this particular case the discrepancy between measurement and calculation is mostly due to the inadequacy of the one-dimensional model of the calculation to treat what actually is a two-dimensional problem. This can be seen quite clearly for the results of σ_{f8}/σ_{f5} which depends on the high energy

flux. In the SNEAK-7B core the mean free path in the high energy region is greater than 4 cm. This should be compared with the pitch of the lattice in SNEAK which is 5.44 cm. The stainless steel and aluminium platelets were contained in only one element. Therefore in the calculational model (infinite slabs) the influence of the steel, or aluminium, is greater than existed in the actual case. This was verified in SNEAK-8 /17/ in which nine elements, in an 3 x 3 array, were loaded with stainless steel platelets so that one had a large slab of steel of thickness 6.4 mm. In the center of this slab the spectral index σ_{F8}/σ_{F5} was measured. The reduction in this index in comparison to a reference measurement without stainless steel was determined to be $7.1 \pm 0.2\%$. The KAPER calculation gave 6.90% with the MOXTOT cross section set and 7.55% with the KFKINR cross section set, the latter having smaller inelastic scattering cross sections for U^{238} than the former.

4.3 Analysis of Reactivity Worth Measurements in SNEAK

Two series of small sample reactivity worth measurements performed in SNEAK have been analyzed with the methods described in this report. These include measurements in SNEAK-5C /11/ and SNEAK-6A /14/, as well as two sodium void measurements in SNEAK-6B /14/.

The assembly 5C of SNEAK was a null-reactivity core with a soft spectrum and strong heterogeneity effects as explained previously. The core consisted of mixed oxide fuel (PuO_2-UO_2), uranium and graphite plates. The sample reactivity measurements were performed in two positions within the unit cell of the core. The unit cell of SNEAK-5C, with the measurement positions shown, is given in Fig. 4.

For comparison with experiment the ratio of the sample worth in position 1 to that in position 2 is used. This eliminates the uncertainty associated with β_{eff} and the absolute magnitude of the normalization integral. These results are given in Table VII. All calculations were performed with the MOXTOT cross section set of Karlsruhe.

The results for SNEAK-5C are also given in Table VI normalized to the reactivity worth of the U^{235} sample. Here the results are compared to a homogeneous diffusion theory perturbation calculation. In this soft spectrum core the sample worths are very position dependent, and therefore, can not be described by a homogeneous calculation.

In Figs. 5 and 6 are given the reactivity worths of U^{238} and Pu^{239} , respectively, as a function of sample thickness. This dependence is quite satisfactorily described by the KAPER program.

One can see that the methods described in this report (KAPER) reproduces the experimental results quite satisfactorily. This is certainly an indication that the procedures used in the KAPER program are valid.

The results of the measurements in SNEAK-6A and calculations with the MOXTOT set are given in Table VIII. The SNEAK-6A unit cell is shown in Fig. 7.

The normalization integral and β_{eff} (0.00421) for the SNEAK-6A results were obtained from a two dimensional diffusion theory calculation.

In general the KAPER results improve the agreement between experiment and calculation. The large Ta sample has a significant heterogeneity effect.

In SNEAK-6B two small sodium void experiments were performed in a bunched cell configuration as shown in Fig. 8. In one experiment the sodium was voided in a fuel material environment and in the other in a structural material environment. The experiment gave a difference in sodium worth in the two environments of more than 30%. The results are given in Table IX as calculated with the MOXTOT cross section set.

It is seen that the KAPER program reproduces the experiment results quite satisfactorily.

5. Conclusions

As it has been demonstrated in the previous sections, the methods employed in the KAPER program are generally adequate for the analysis of measurements performed in a heterogeneous environment of fast critical assemblies.

The application of the "f-factor concept" to heterogeneous calculations, in slab geometry, has been shown to be consistent with its use in homogeneous calculations. Whereas this procedure is not as accurate as the methods used in ultrafine group slowing-down code it certainly yields a sufficient accuracy for routine calculations.

The flexibility of the program in treating local perturbations in the normal unit cell is valuable in the analysis of many experiments since the measurements themselves many times introduce a disturbance in the cell. The adequacy of the procedures in the program for treating these problems has been sufficiently demonstrated.

Finally, the use of the KAPER program for the interpretation of small-sample reactivity worth measurements significantly

improves our understanding of these measurements. This is demonstrated particularly for the case when one calculates the worth for the same sample in difference positions, or environments. The ratio of these two calculations eliminates the uncertainties associated with β_{eff} and the normalization integral. We have then a direct test of the calculation of the sample cross sections and the local flux and adjoint.

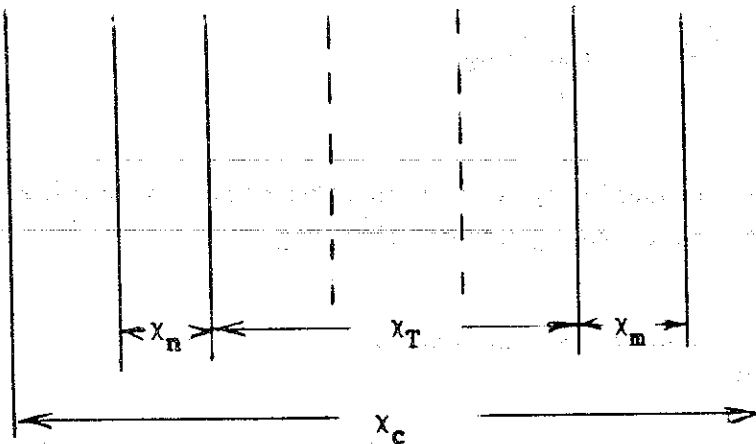
APPENDIX

Methods used for the calculation of collision probabilities

If one integrates the first-flight collision probability $p(\bar{r}' \rightarrow \bar{r})$, as given by Eq. (2.1a), in slab geometry, one encounters exponential integrals of order 3

$$E_3(\chi) = \int_0^1 dt e^{-\chi/t} t$$

Consider the case of calculating the probability a neutron from region n collides in region m of the same cell. In the simplified sketch below of a cell



of optical thickness x_c , where

$$x_c = \sum_i \Sigma_{t_i} d_i$$

Σ_{c_i} = total cross section of region i (cm^{-1})

d_i = thickness of region i (cm)

one can easily calculate P_{nm} to be

$$P_{nm} = 1/2\chi_n \{ E_3(\chi_T) - E_3(\chi_n + \chi_T) - E_3(\chi_T + \chi_m) + E_3(\chi_n + \chi_T + \chi_m) \} \quad (\text{A.1})$$

However the collision probabilities in Eqs. (2.20) and (2.21), as stated in their definition, must include the probability the neutron from region n collides in all regions m of the surrounding cells. Therefore we must sum over of regions m of the surrounding cells

$$P_{nm} = \sum_{j=0}^{\infty} P_{nj_m} \quad (\text{A.2})$$

where P_{nj_m} = probability a neutron from region n collides in region m of the j^{th} cell.

For $j=0$, P_{nj_m} is equal to Eq. (A.1).

We have therefore an infinite sum of exponential integrals. These infinite sums are evaluated by utilizing a special Gauss quadrature formula /15/ of the form

$$\sum_{n=0}^{\infty} E_n(\chi + \chi_c n) = \sum_{i=1}^4 w_i \exp(-\chi t_i) \quad (\text{A.3})$$

where w_i are the weights and t_i are the modes. The error in this formula is of the order of $<10^{-5}$. With this formula one is able to evaluate the collision probabilities quite rapidly with reasonable accuracy.

References

- /1/ P. Engelmann et al.
"Construction and Experimental Equipment of the Karlsruhe Fast Critical Facility, SNEAK"
Kernforschungszentrum Karlsruhe, KFK-471 (1966)
- /2/ D. Wintzer
"Zur Berechnung von Heterogenitätseffekten in periodischen Zellstrukturen thermischer und schneller Kernreaktoren"
Kernforschungszentrum Karlsruhe, KFK-743 (1969). See also
"Heterogeneity Calculations including Space-Dependent Resonance Self-Shielding" in Proceedings of a IAEA Symposium Fast Reactor Physics Karlsruhe, November 1967
- /3/ I.I. Bondarenko et al.
"Group Constants for Nuclear Reactor Calculations"
Consultants Bureau, New York (1964)
- /4/ W.J. Oosterkamp
"The Measurement and Calculation of the Reactivity Worth of Samples in a Fast-Heterogeneous Zero Power Reactor"
Kernforschungszentrum Karlsruhe, KFK-1036 (1969)
- /5/ E.A. Fischer
"The Overlap Effect of Resonances of Different Fuel Isotopes in the Doppler-Coefficient Calculations for Fast Reactors"
Nukleonik 8, 146 (1966)
- /6/ P. Benoist
"Théorie du coefficient de diffusion des neutrons dans un réseau comportant des cavités"
CEA-R-2278 (1964)

- /7/ R.A. Karam et al.
"Analysis of Central Reactivity Worths in Fast Critical Assemblies"
Nuclear Science and Engineering, Vol. 40, 414-423 (1970)
- /8/ P. Mc Grath and W.K. Foell
"Integral Transport Theory Analysis of Central Reactivity Worth Measurements"
Nuclear Science and Engineering, Vol. 45, 237-244 (1971)
- /9/ E.A. Fischer
"A Method to Calculate Reactivity Worth by Integral Transport Theory"
Kernforschungszentrum Karlsruhe, KFK-995 (1969)
- /10/ A. Khairallah and F. Storrer
"Calculation of the Sodium-void and Doppler Reactivity Coefficients in Fast Reactors and Critical Assemblies, with Heterogeneities Taken into Account"
Proceedings of the International Conference on Fast Critical Experiments and Their Analysis, Argonne National Laboratory, ANL-7320, 394-402 (1966)
- /11/ K. Böhnelt and H. Meister
"A Fast Reactor Lattice Experiment for Investigation of k_{∞} and Reaction Rate Ratios in SNEAK, Assembly 5"
Kernforschungszentrum Karlsruhe, KFK-1176 (1970)
- /12/ E. Kiefhaber, unpublished note (1969)
- /13/ R. Schröder
"Physics Investigations of Uranium-Fueled Fast Steam-Cooled Reactors in SNEAK, Assemblies 3A-0, 3A-2, 3A-3"
Kernforschungszentrum Karlsruhe, KFK-847 (1968)

- /14/ Projekt Schneller Brüter, 2. Vierteljahresbericht 1970
Kernforschungszentrum Karlsruhe, KFK-1270/2
Section 121, pgs. 18-40 (1970)
- /15/ A.P. Olson
Mathematics of Computation, Vol. 23, 106 (1969)
- /16/ Projekt Schneller Brüter, 2. Vierteljahresbericht 1971
Kernforschungszentrum Karlsruhe, KFK-1271/2
Section 121, pgs. 10-13 (1971)
- /17/ Projekt Schneller Brüter, 3. Vierteljahresbericht 1971
Kernforschungszentrum Karlsruhe, KFK-1271/3
Section 121, pgs. 25-28 (1971)

Table Ia

Atomic Densities for the SNEAK-5C Simplified
Cell (in 10^{20} cm^{-3})

Composition No.	C 12	CR 52	Fe 56	O 16	Pu ²³⁹	U ²³⁸
1	0	42.5	99.4	325.9	39.35	118.76
2	0	26.9	39.5	0	0	390.0
3	777.5	16.8	39.5	0	0	0

Table Ib

Thickness of Plates for the SNEAK-5C Simplified Cell

Region No.	Thickness, cm	Composition No.
1	2.08	3
2	1.00	3
3	0.157	2
4	0.15	1
5	0.328	1
6	0.15	1
7	0.157	2
8	0.157	2
9	1.00	3

Table II

 k_{∞} for the SNEAK-5C Simplified Cell

Relative Thickness of the cell	ZERA		KAPER	
	k_{∞}	δk	k_{∞}	δk
10^{-3} (quasi homogeneous)	0.9342	--	0.9343	--
1/4	0.9640	0.0298	0.9627 (0.9628) ⁺	0.0284
1/2	0.9849	0.0507	0.9828 (0.9825)	0.0485
Full	1.0156	0.0814	1.0101 (1.0094)	0.0758

⁺) k_{∞} values in parentheses are values before iteration on the source densities

Table III Dependence of k_{∞} on the background cross section due to U²³⁸

	SNEAK-5C, ZERA / 12/			Simplified SNEAK-5C, KAPER		
	k_{HOM}	k_{HET}	δk	k_{HOM}	k_{HET}	δk
Self-shielded with σ_{p8}	0.9340	1.0016	+0.0676	0.9343	1.0101	0.0758
Self-shielded with σ_{t8}	0.9404	0.9504	+0.0100	0.9414	1.0211	0.0797

Table IV

Dependence of the effective cross sections of Pu²³⁹
on the background cross section due to U²³⁸ (KAPER)
(SNEAK-5C simplified cell, region 5)

	Background cross section of U ²³⁸ , b	Self-shielded cross sections of Pu ²³⁹			
		σ_{f9}	% difference	σ_{c9}	% difference
<u>Group 14 (1.00 - 2.15 keV)</u>					
Infinite Dilution	-	3.929			
Self-shielded with σ_{p8}	10.6	3.778	-3.8	2.192	-5.7
Self-shielded with σ_{t8}	19.9	3.794	+0.4	2.206	+0.6
<u>Group 16 (215 - 465 eV)</u>					
Infinite Dilution	-	12.48	-	8.63	
Self-shielded with σ_{p8}	10.6	10.91	-12.8	6.72	-22.1
Self-shielded with σ_{t8}	20.3	11.06	+1.4	6.87	+2.2
<u>Group 18 (46.5 - 100 eV)</u>					
Infinite Dilution	-	54.5		50.8	
Self-shielded with σ_{p8}	10.6	31.8	-42	21.6	-57
Self-shielded with σ_{t8}	40.2	34.0	+7	23.9	+10

Table V
 k_{eff} for SNEAK-3A-2, assuming $B^2 = 0.0024 \text{ cm}^{-2}$
 (SNEAK cross section set)

Cell Thickness, cm	ZERA		KAPER	
	k_{eff}	δk	k_{eff}	δk
1.256×10^{-3} (quasi hom.)	0.9960	---	0.9972	---
1.256 heterog.	0.9987	0.0027	0.9986	0.0014
2.512 bunched	0.9994	0.0034	0.9986 (0.9984) ⁺	0.0014
5.024 double bunched	0.9992	0.0032	0.9973 (0.9967)	0.0001

⁺) k_{eff} values in parentheses are values before iteration on the source densities

Table VI

Reactivity Worths in SNEAK-5C

Sample	Sample weight gm	Position	Experiment $\mu\$/gm$	Calculation / Exp.	
				Homogeneous ^{*)}	KAPER
U ²³⁵	3	1	435 \pm 4.	1.0	1.0
Pu ²³⁹	5	1	443 \pm 5.	.96	1.08
Pu ²³⁹	5	2	390 \pm 5.	1.09	1.07
U ²³⁸	5	1	-86 \pm 3.	.35	.97
U ²³⁸	5	2	-25 \pm 3.	1.21	1.07
U ²³⁸	60	1	-37.7 \pm 4.	.80	1.09
U ²³⁸	60	2	-24.4 \pm 3.	1.24	1.09
Pu ²⁴⁰	3	1	-170 \pm 5.	.78	.96
Pu ²⁴⁰	3	2	-104 \pm 5.	1.27	1.19
Fe ₂ O ₃	3	1	-22 \pm 5.	.70	.48
Fe ₂ O ₃	3	2	-50 \pm 5.	.31	.50

^{*)} Homogeneous one-dimensional diffusion theory perturbation

Table VII

Reactivity Worth Ratios in SNEAK-5C

Position 1 / Position 2	Sample Weight [g]	Experiment	Calculation KAPER
Pu ²³⁹	5	1.135	1.146
U ²³⁸	5	3.440	3.127
U ²³⁸	60	1.545	1.540
Pu ²⁴⁰	3	1.635	1.310
Fe ₂ O ₃	3	.440	.430

Table VIII

Material Worth in SNEAK-6A

	Sample weight g	Experiment $\mu\$/g$	Calculation / Exp.	
			Diffusion	KAPER
U ²³⁵	3.3	512 \pm 10	1.22	1.19
U ²³⁸	62.	-33.2 \pm 0.5	1.25	1.19
Pu ²³⁹	4.	740 \pm 7	1.05	1.03
Pu ²⁴⁰	2.7	107 \pm 10	.99	.97
SS	17.	-27.2 \pm 2	.89	.90
Fe ₂ O ₃	3.	-10. \pm 10	3.1	3.1
B ₄ C	6.	-1720 \pm 5	1.11	1.04
Eu ₂ O ₃	4.	-705 \pm 8	.91	.88
Ta	220.	-143 \pm 0.2	1.90	1.07
Na	30.	-31.3	1.14	1.38

Table IX

Na-void in SNEAK-6B ($\mu\$/g$)

	Experiment	KAPER
Na in fuel	-25.5	-31.33
Na in structural material	-19.0	-23.70
Ratio: fuel / structural material	1.342	1.322

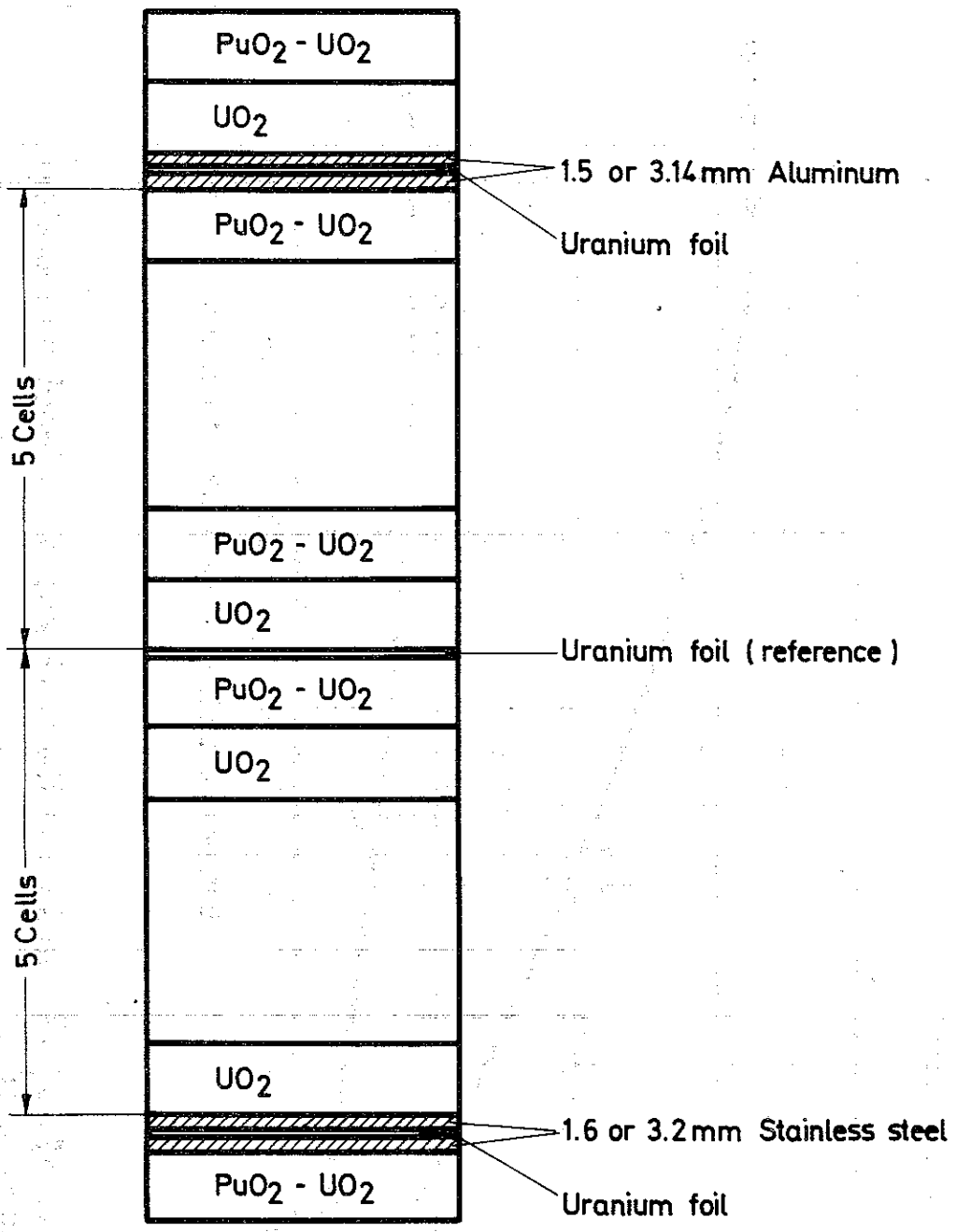


Fig.1 Spectral indices measurements in SNEAK-7B

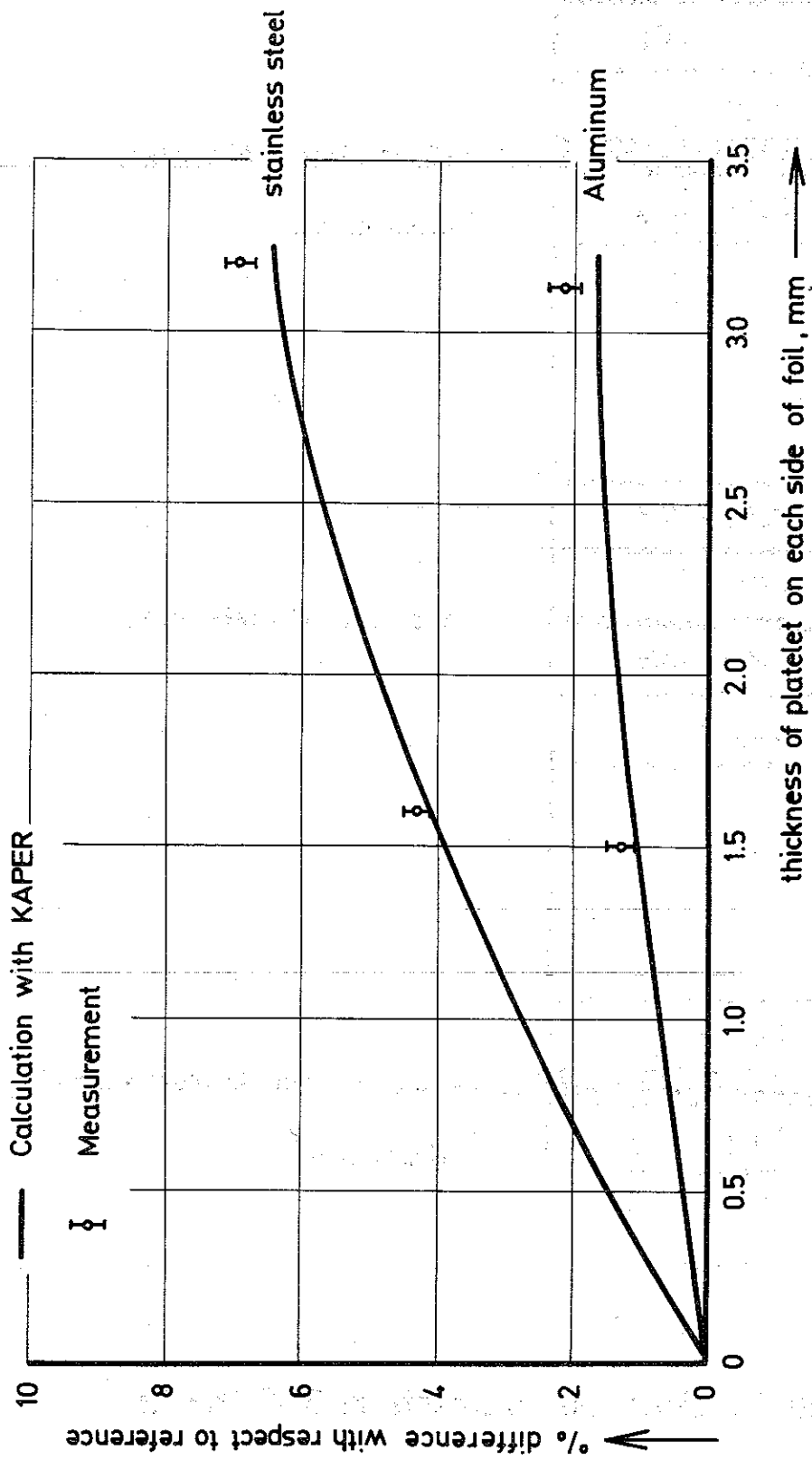


Fig.2 Change in σ_c^8 / σ_f^5 as function of the thickness of material surrounding foil, SNEAK - 7B

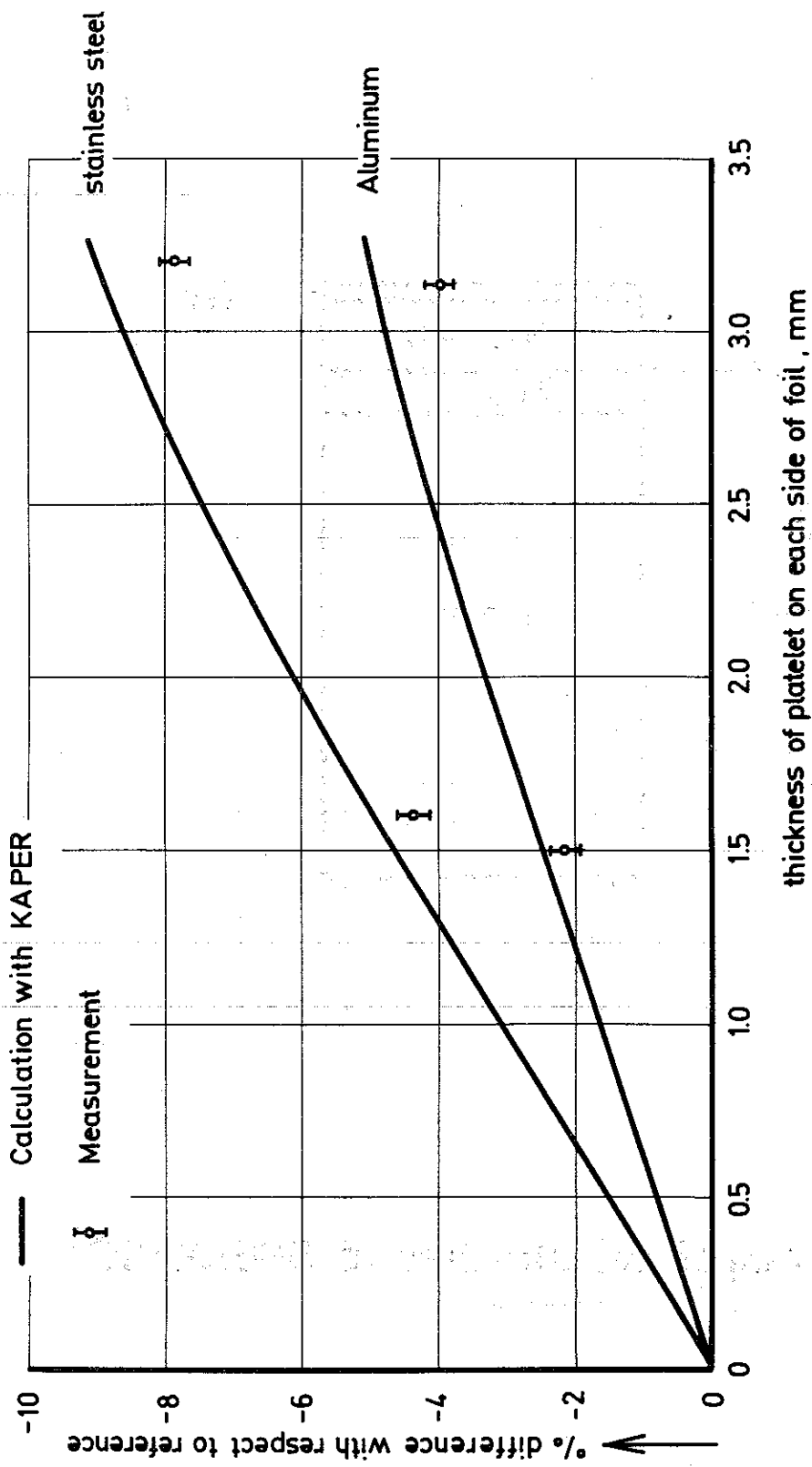


Fig.3 Change in σ_f^8 / σ_f^5 as function of the thickness of material surrounding foil, SNEAK - 7B

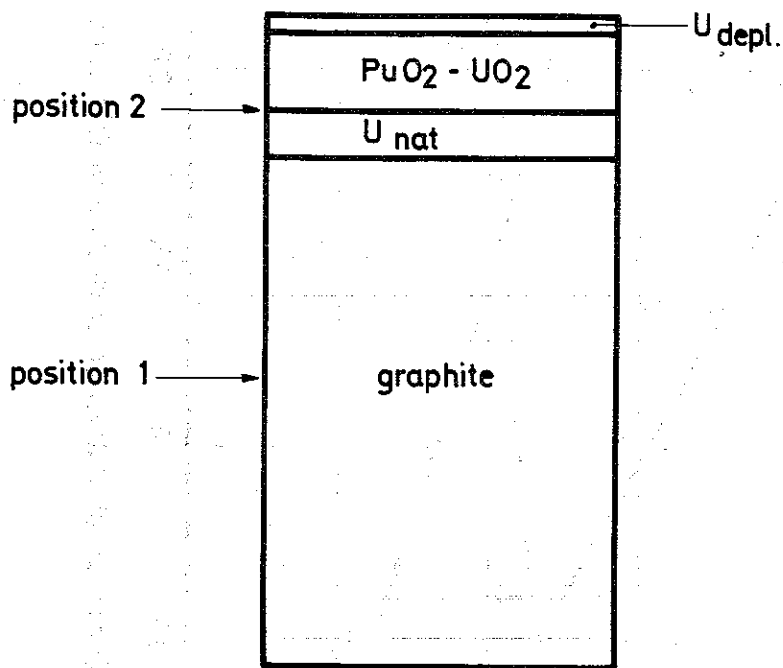
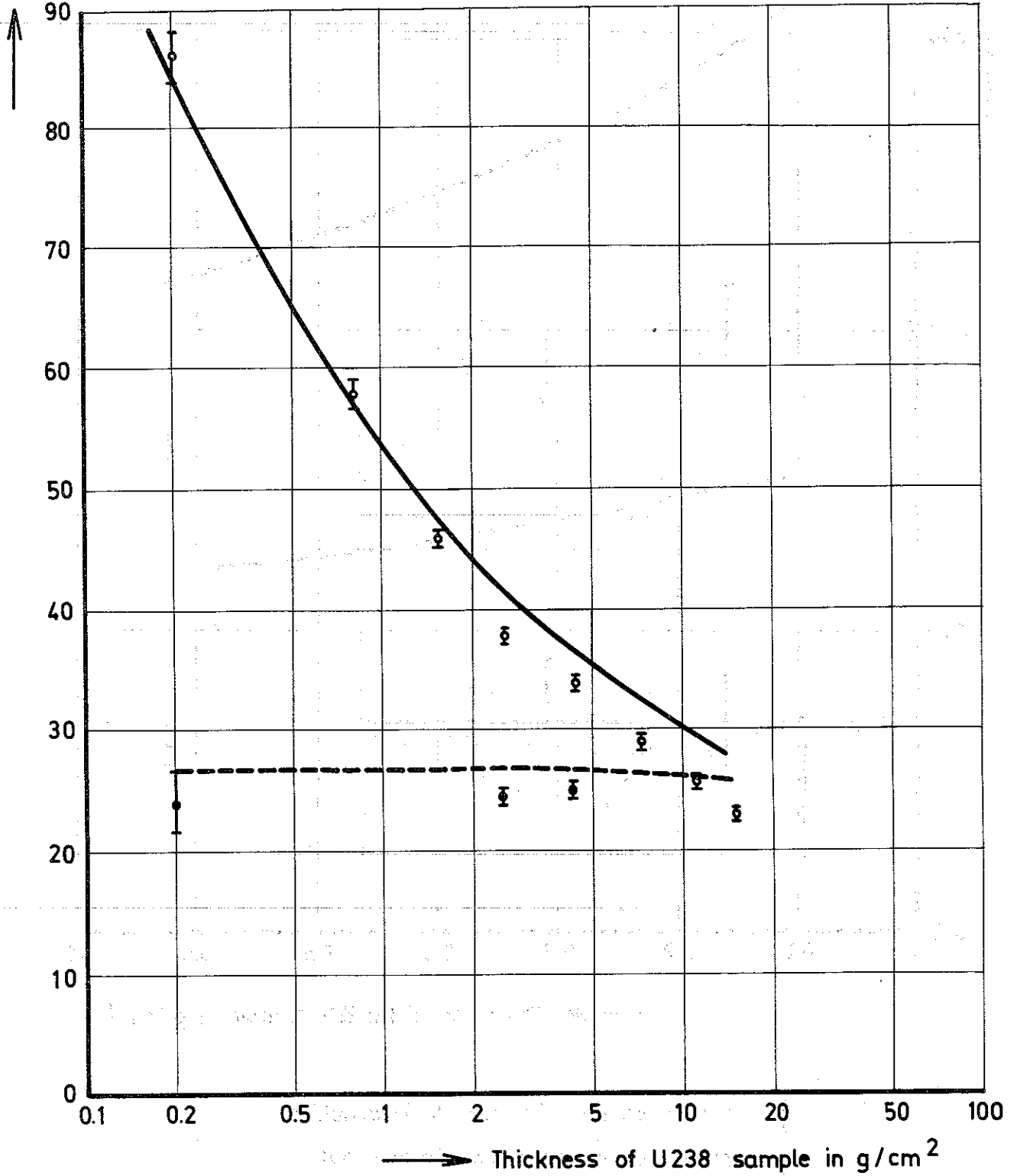


Fig.4 Principal cell structure of SNEAK-5C

$-\Delta\rho$ ($\mu\$/g$)







-  measurement with sample in graphite
-  measurement with sample in U nat
-  sample in graphite
-  sample in U nat
- } heterogeneous perturbation calculation with MOXTOT set

Fig.5 Central Reactivity Worth of U238 in SNEAK-5C

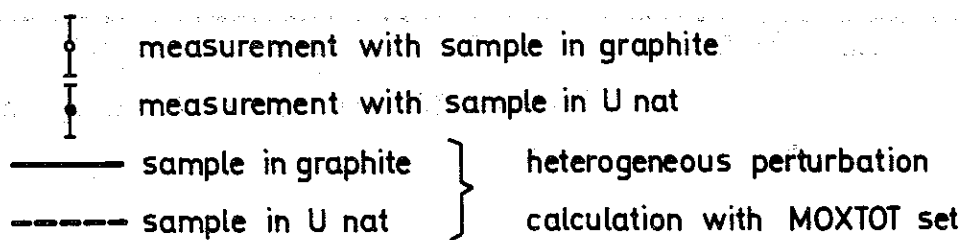
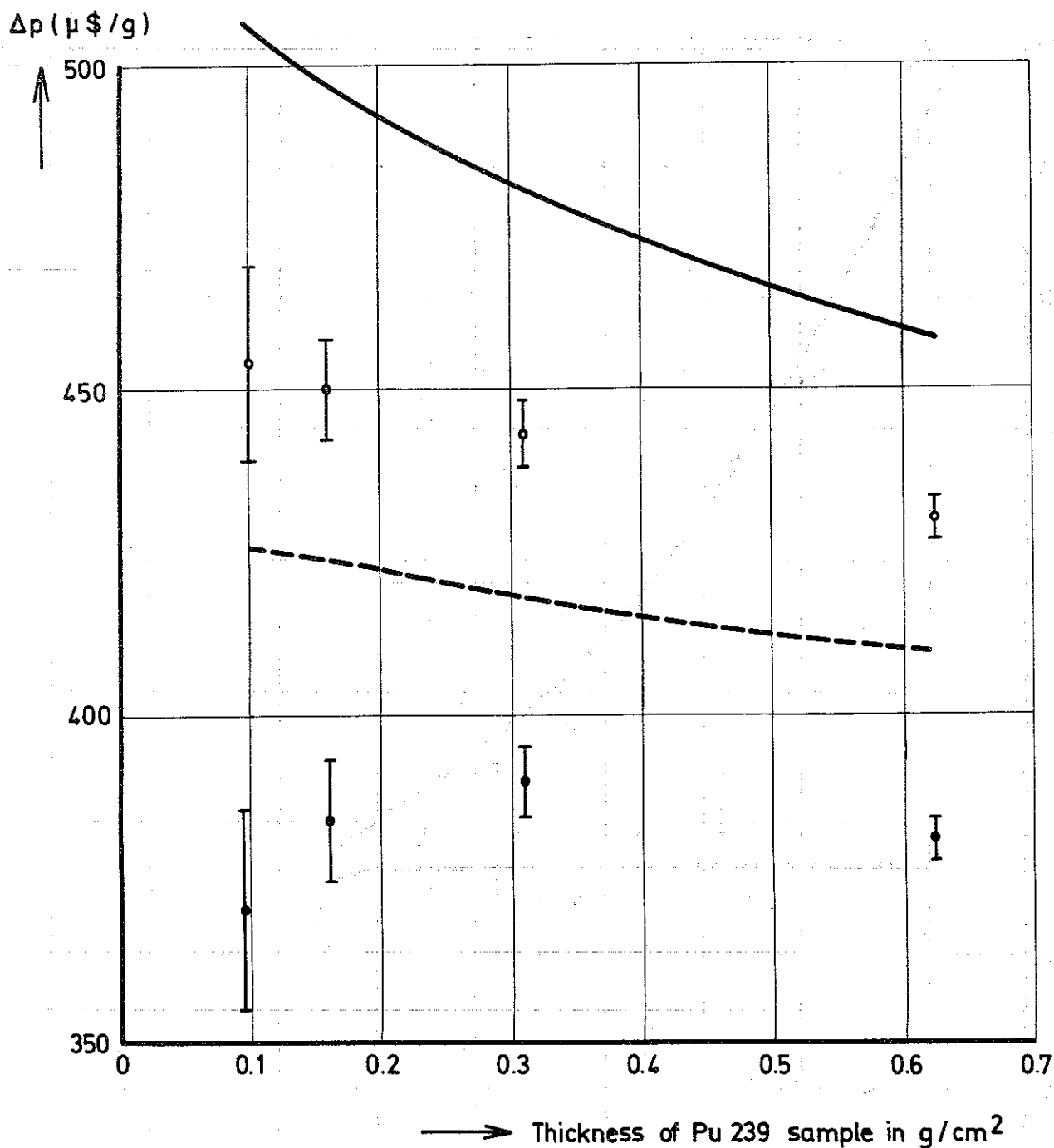


Fig.6 Central Reactivity Worth of Pu 239 in SNEAK-5C

Na	
U nat	SS 25%
Na	
PuO ₂ UO ₂	
Ferrit	
Na	
PuO ₂ UO ₂	
Na	SS 100%
	U depl.
Na	
PuO ₂ UO ₂	

Fig.7 Unit cell of SNEAK - 6A

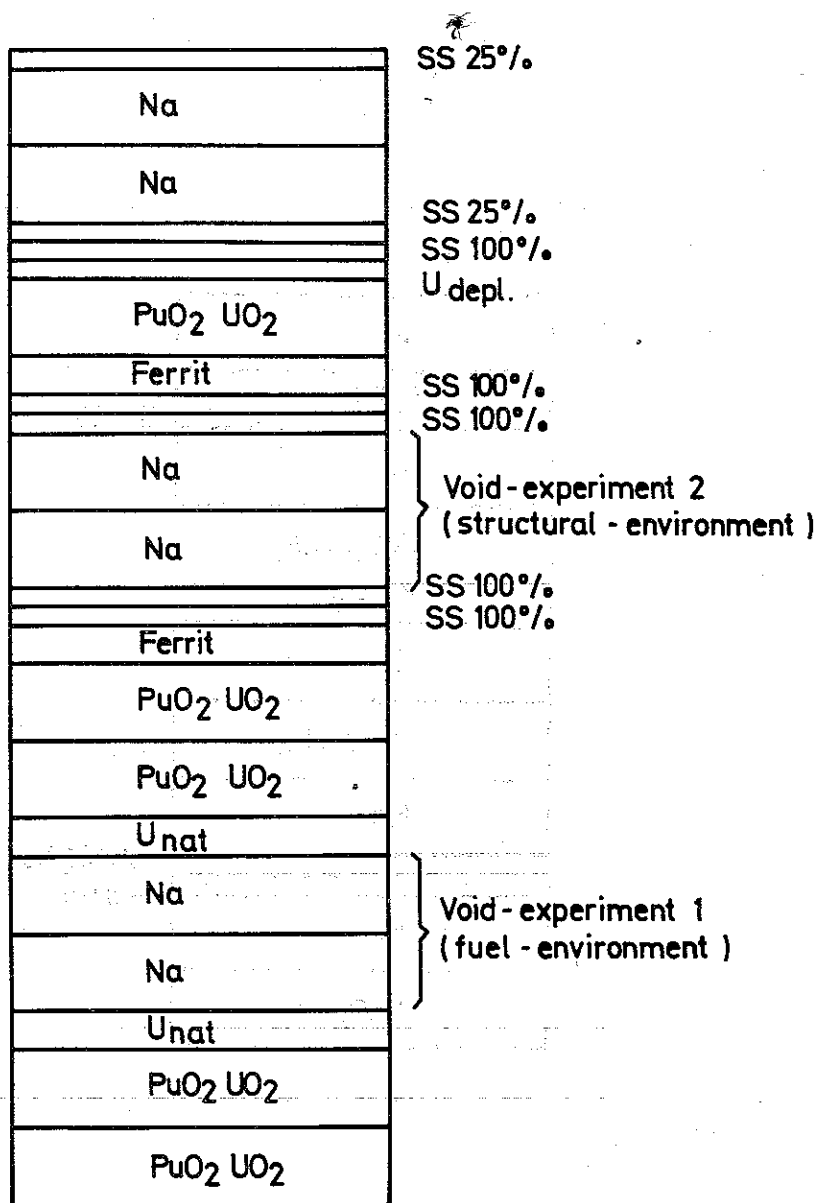


Fig.8 Bunched cell in SNEAK - 6B
(for Na - Void - experiment)